Endoplasmic reticulum targeted chemotherapeutics: remarkable photo-cytotoxicity of oxovanadium(IV) vitamin-B6 complex in visible light †

Samya Banerjee,[a] Akanksha Dixit,[b] Radhika N. Shridharan,[b] Anjali A. Karande,*[b] and Akhil R. Chakravarty*[a]

[a] *Department of Inorganic and Physical Chemistry, Indian Institute of Science and* [b] *Department of Biochemistry, Indian Institute of Science, Bangalore 560012, India. E-mail: arc@ipc.iisc.ernet.in; anjali@biochem.iisc.ernet.in*

Electronic Supplementary Information (ESI)

Experimental Section

Materials and measurements

All the reagents and chemicals were procured from commercial sources (s.d. Fine Chemicals, India; Aldrich, USA) and used as such. Pyridoxal hydrochloride was purchased from Sigma-Aldrich. Solvents were purified by standard procedures.[S1] Dulbecco's Modified Eagle's medium (DMEM), propidium iodide, Hoechst 33342, 3-(4,5-dimethylthiazol-2-yl)-2,5-diphenyltetrazolium bromide (MTT) and 2',7'-dichlorofluorescein diacetate (DCFDA) were procured from Sigma-Aldrich (USA). ER-Tracker Red was bought from Invitrogen (U.S.A.). 11-(9-Acridinyl)dipyrido[3,2-a:2′,3′-c]phenazine (acdppz) ligand was prepared following a literature procedure using 1,10-phenanthroline-5,6-dione as a precursor.[S2] The Schiff base ligand, 3-hydroxy-5-(hydroxymethyl)-4-(((2-hydroxyphenyl)imino)methyl)-2-methylpyridin-1-ium chloride ($H_2L.HCl$) was synthesized following the literature procedure by reacting pyridoxal hydrochloride with 2-aminophenol in dry methanol at room temperature.[S3] Synthesis of the complexes was carried out under nitrogen atmosphere using Schlenk technique. Tetrabutylammonium perchlorate (TBAP) was prepared using tetrabutylammonium bromide and perchloric acid.

The elemental analysis was done using a Thermo Finnigan FLASH EA 1112 CHNS analyzer. The infrared and electronic spectra were recorded on Perkin Elmer Lambda 35 and Perkin Elmer spectrum one 55, respectively, at 25 °C. Molar conductivity measurements were done using a Control Dynamics (India) conductivity meter. Electrochemical measurements were made at 25 °C on an EG&G PAR model 253 VersaStat potentiostat/galvanostat with electrochemical analysis software 270 using a three electrode setup consisting of a glassy carbon

working, platinum wire auxiliary and a saturated calomel reference electrode (SCE) in 20% DMF in Tris buffer. Tetrabutylammonium perchlorate (TBAP) (0.1 mol) was used as a supporting electrolyte for the electrochemical measurements. Electrospray ionization mass spectral measurements were done using Agilent Technologies 6538 UHD Accurate-mass Q-TOF LC/MS Mass spectrometers. The NMR spectra were recorded using Bruker Avance 400 (400 MHz) NMR spectrometer. Room temperature magnetic moment of the DMSO-d_6 solutions of the oxovanadium(IV) complexes containing 1% TMS (v/v) as the internal reference was obtained by a solution NMR method with a Bruker AMX-400 NMR spectrometer.[S4] Room temperature fluorescence quantum yield measurement was done using a Perkin-Elmer LS 55 fluorescence spectrometer using coumarin-153 laser dye as a reference with a known Φ value of 0.56 in acetonitrile.[S5] Samples were deaerated prior to spectral measurements. The complex and reference were excited at 390 nm, maintaining nearly equal absorbance and the emission spectra were recorded from 410 to 650 nm. The integrated emission intensity was calculated using Origin Pro 8.1 software and the quantum yield was calculated using the equation: $(\Phi_S/\Phi_R) = (A_S/A_R)x((OD)_S/(OD)_R)x(n_S^2/n_R^2)$, where Φ_S and Φ_R are the fluorescence quantum yields of the sample and reference respectively, A_S and A_R are the area under the fluorescence spectra of the sample and the reference respectively, $(OD)_S$ and $(OD)_R$ are the respective optical densities of the sample and the reference solution at the wavelength of excitation, and n_S and n_R are the refractive indices for the respective solvents used for the sample and the reference.[S6,S7] For the direct measurement of quantum yield for singlet oxygen production of complex **2** through the NIR luminescence method, we used a Fluorolog 3 spectrofluorimeter (FL3-221) connected with a NIR detector (Hamamatsu H10330A-45) and 450 W xenon lamp as the light source. To obtain the direct singlet oxygen luminescence intensity in the steady-state method, we prepared

optically matched methanolic solutions of complex **2** and the reference hematoporphyrin (Hp). Excitation at 440 nm, we obtained the luminescence maxima at 1273 nm which corresponds to singlet oxygen.[S8,S9] From the emission intensities of complex **2** and Hp, the singlet oxygen quantum yield (Φ_{Δ}) was calculated by the equation: $\Phi_{\Delta S}=(I_R/I_S)\times(I_{\Delta S}/I_{\Delta R})\times(\tau_R/\tau_S)\times\Phi_{\Delta R}$, where I_S and I_R represent the incident light intensity and $I_{\Delta S}$ and $I_{\Delta R}$ represent the singlet oxygen luminescence intensity at 1273 nm for complex **2** and the reference, respectively. The τ_R and τ_S represent the singlet oxygen phosphorescence lifetimes of reference and sample in a particular solvent, and $\Phi_{\Delta R}$ is the singlet oxygen quantum yield of the reference, Hp. Fluorescence microscopic investigations were carried out using fluorescence microscope of Carl Zeiss (Germany) make. Flow cytometric analysis was performed using FACS Calibur (Becton Dickinson (BD) cell analyzer) at FL1 channel (595 nm).

Preparation of [VO(HL)(bpy)]Cl (1) and [VO(HL)(acdppz)]Cl (2):

Vanadyl sulfate (0.16 g, 1.0 mmol) and barium chloride (0.25 g, 1.0 mmol) together were dissolved in 15 ml of EtOH and 3 ml of water. The mixture was then stirred at room temperature for 1.5 h under inert atmosphere of nitrogen using Schlenk technique. The mixture was filtered using celite to remove white barium sulphate precipitate. The blue filtrate was deaerated and then saturated with nitrogen. An ethanolic solution (15 ml) of the corresponding polypyridyl base (0.15 g, bpy; 0.46 g, acdppz, (1.0 mmol)) was added to the filtrate. A deep greenish solution was formed after stirring the mixture for 15 min. To this mixture was added a deaerated ethanol solution (25 ml) of the vitamin-B6 Schiff base ligand as hydrochloride salt (0.25 g, 1.0 mmol). The complexes were precipitated out after refluxing the resulting solution for 1 h as brick red

solid. The precipitate was then filtered, isolated and washed with ethanol, THF and chloroform and finally dried in vacuum over P_4O_{10} [Yield: ~ 81% for **1** and ~ 76% for **2**].

Characterization data

Complex **1**: Anal. Calcd for $C_{24}H_{21}N_4ClO_4V$: C, 55.88; H, 4.10; N, 10.86. Found: C, 55.69; H, 4.13; N, 10.90. ESI-MS in CH_3OH: m/z 480.1046 $[M]^+$. IR data (KBr phase, cm^{-1}): 3449 br, 1604 vs (C=N), 1531 m, 1463 m, 1401 m, 1318 m, 1208 w, 1172 w, 1120 w, 1031 m, 957 s (V=O), 837 m, 732 m, 626 w, 531 m (br , broad; vs, very strong; s, strong; m, medium; w, weak). UV-visible in 10% DMF [λ_{max}/nm (ε/ dm^3 mol^{-1} cm^{-1})]: 770 (52), 441 (15 200), 277 (48 200). Λ_M = 78 S m^2 mol^{-1} in DMF at 25 ºC. μ_{eff}, μ_B at 298 K: 1.63.

Complex **2**: Anal. Calcd for $C_{45}H_{30}N_7ClO_4V$: C, 65.98; H, 3.69; N, 11.97. Found: C, 65.71; H, 3.74; N, 11.88. ESI-MS in CH_3OH: m/z 783.1874 $[M]^+$, IR data (KBr phase, cm^{-1}): 3678 br, 1605 s (C=N), 1530 m, 1477 w, 1462 m, 1420 w, 1354 w, 1152 m, 1075 w, 955 s (V=O), 838 m, 736 m, 534 m. UV-visible in 10% DMF [λ_{max}/nm (ε/ dm^3 mol^{-1} cm^{-1})]: 751 (65), 439 (13 700), 390 (27 600), 362 (23 100), 270 (72 800). Λ_M = 73 S m^2 mol^{-1} in DMF at 25 ºC. μ_{eff}, μ_B at 298 K: 1.61.

Solubility and stability

The complexes showed good solubility in DMF, DMSO, methanol and acetonitrile and moderate solubility in water and ethanol. They had poor solubility in hydrocarbons. They were stable in both solid and solution phases.

X-ray crystallographic procedures

The crystal structure of complex **1** as its perchlorate salt, viz. **1a**·EtOH, was obtained by single crystal X-ray diffraction method. Crystals were obtained on slow evaporation of an acetonitrile-methanol (2:3 v/v) solution of the complex. Crystal mounting was done on glass

fibre with epoxy cement. All geometric and intensity data were collected using an automated Bruker SMART APEX CCD diffractometer equipped with a fine focus 1.75 kW sealed tube Mo-K_α X-ray source (λ = 0.71073 Å) with increasing ω (width of 0.3° per frame) at a scan speed of 5 sec per frame. Intensity data, collected using ω-2θ scan mode, were corrected for Lorentz–polarization effects and for absorption.[S10] The structure was solved and refined using SHELXL97[S11] present in the WinGx suit of programs (Version 1.63.04a).[S12] All non-hydrogen positions were initially located in the difference Fourier maps, and for the final refinement, the hydrogen atoms were placed in geometrically ideal positions and refined in the riding mode. The hydrogen atom attached to the pyridoxal nitrogen atom was located in the difference Fourier map. Final refinement included atomic positions for all the atoms, anisotropic thermal parameters for all the non-hydrogen atoms and isotropic thermal parameters for all the hydrogen atoms. Perspective view of the molecule was obtained by ORTEP.[S13] Selected bond distances and angles in the complex are given in Table S1.

Computational methodology

To rationalize the photophysical properties of the complexes, computational studies were performed for both the complexes using B3LYP/LANL2DZ level of DFT.[S14] The hybrid U3LYP functional and LANL2DZ basis set were used in all calculations as incorporated in Gaussian 09 package.[S15] Visualizations of the optimized structures and the MOs were performed using Gaussview5.0. To ascertain stationary points, further frequency test was performed.

Cell cytotoxicity assay

HeLa and MCF-7 cancer cells and MCF-10A normal cells were analyzed for viability post treatment using the MTT assay. The photocytotoxicity of the complexes was based on the ability of mitochondrial dehydrogenases in the viable cells to cleave the tetrazolium rings of

MTT 3-(4,5-dimethylthiazol-2-yl)-2,5-diphenyltetrazolium bromide to form dark blue membrane impermeable crystals of formazan, which upon solubilization can be measured spectrophotometrically.[S16] Approximately 15 x 10^3 HeLa cells, 15 x 10^3 MCF-7 cells and 1 x 10^4 MCF-10A cells were plated in a 96-well culture plate in DMEM supplemented with 10% fetal bovine serum (10% DMEM) and cultured overnight. The stock solutions of the complexes **1**, **2** and the ligands that were prepared in DMSO were first diluted in the culture medium to the desired concentration and then added to the cells in 96 well plates. The final concentration of DMSO was kept constant at 1% for all tests. Then cells were incubated for 4 h in the dark. To examine the dark toxicity of complex **2** over a prolonged period of time, cells were incubated for 24 h and 48 h in dark. The medium was then replaced with 50 mmol phosphate buffer (pH 7.4) containing 150 mmol NaCl (PBS) and cells were photo-irradiated for 1 h in visible light of 400-700 nm using Luzchem Photoreactor (Model LZC-1, Ontario, Canada) fitted with Sylvania make 8 fluorescent white tubes with a fluence rate of 2.4 mW cm^{-2} to provide a total dose of 10 J cm^{-2}. PBS was replaced with 10% DMEM after irradiation and cells were incubated for a further period of 20 h in dark. Post incubation, 25 µl of MTT (4 mg ml^{-1} in PBS) was added to each well and incubated for 3 h. The culture medium was discarded and 200 µl of DMSO was added to dissolve the formazan crystals. The intensity of the dark blue colour formed by the formazan complex was estimated at an absorbance of 540 nm using an ELISA microplate reader (BioRad, Hercules, CA, USA). The cytotoxicity of the test compounds was measured as the percentage ratio of the absorbance of the treated cells over the untreated controls. The IC_{50} values were determined by nonlinear regression analysis (GraphPad Prism). For confirming that the complex **2** was taken up by cells mainly through VB6 transporting membrane carrier (VTC) mediated

diffusion, HeLa cells were first incubated with 4 mM vitamin B6 for 45 min with subsequent addition of complex **2** for the MTT assay.

DNA fragmentation analysis by agarose gel electrophoresis

DNA fragmentation analysis was conducted to determine the mechanism of cell death induced by complex **2**. Briefly, $0.3x10^6$ HeLa and MCF-7 cells were plated separately in 60 mm dish. The cells were cultured for 24 h and incubated for 4 h in dark with **2** (1 μM in HeLa and 2 μM in MCF-7). One dish containing the complex was exposed to light for 1 h and again the cells were incubated for 4 h along with its dark control. After 4 h, cells were trypsinized, washed with DPBS, re-suspended in 0.4 ml of lysis buffer (10 mM Tris-HCl; pH, 8.0, 20 mM EDTA, 0.2% triton-X 100) and kept on ice for 20 min. The lysed cells were centrifuged for 20 min at 13000 rpm and their supernatants (which had soluble chromosomal DNAs including both high molecular weight DNA and nucleosomal DNA fragments) were collected. Phenol chloroform extraction was carried out to remove proteins. Later, the supernatant was precipitated with 1/10 volume of 3M sodium acetate (pH, 5.8) and 2 volumes of ethanol at –20 °C for overnight. The precipitated DNA was washed with 70% alcohol and re-suspended in Tris-EDTA (pH 8) containing RNAse (100 μg/ml RNAse) followed by incubation at 37 °C for 2 hrs. The DNA samples were resolved on 1.5% agarose gel at 80 V for approximately 2 h and photographed under UV light.

Annexin-V FITC and Propidium Iodide (PI) assay

To confirm the apoptotic pathway of cell death, HeLa (4×10^5 cells/ml) and MCF-7 (4×10^5 cells/ml) cells were treated with complex **2** (1 μmol in HeLa and 2 μmol in MCF-7) in 10%

DMEM for 4 h, followed by exposure to visible light for 1 h. The cells were then cultured for 18 h in complete medium, harvested and washed twice with chilled PBS at 4°C. The cells were re-suspended in 100 ml Annexin-V binding buffer (100 mmol HEPES/ NaOH, pH 7.4 containing 140 mmol NaCl and 2.5 mmol $CaCl_2$), stained with Annexin-V FITC and PI, and incubated for 15 min at RT in the dark. After incubation, 400 µl of binding buffer was added to the cells and analyzed immediately using flow cytometry.[S17]

DCFDA assay for measurement of ROS generation

The generation of any reactive oxygen species (ROS) was probed using 2',7'-dichlorodihydrofluorescein diacetate (DCFDA) assay.[S18] Cell permeable DCFDA can be oxidized by cellular ROS to generate fluorescent DCF with an emission maxima at 525 nm.[S19] The percentage of cells generating ROS can be determined by flow cytometry analysis. To detect ROS generation, HeLa cells were incubated with complex **2** (1 µmol) for 4 h followed by photo-irradiation (400-700 nm) for 1 h in 50 mmol PBS. The cells were harvested by trypsinization and single cell suspension of $1x10^6$ cells ml^{-1} was prepared. The cells were then treated with 10 µmol DCFDA solution in DMSO in dark for 15 min at room temperature. The distribution of DCFDA stained HeLa cells was determined by flow cytometry.

Cellular incorporation assay

Flow cytometric analysis was performed to study the rate of uptake of complex **2** into HeLa, MCF-7 cancer cells and MCF-10A normal cells. Approximately $0.3x10^6$ cells were plated per well of a 6-well tissue culture plate in Dulbecco's Modified Eagle Medium (DMEM) containing 10% FBS. After 24 h of incubation at 37 °C in a CO_2 incubator, complex **2** (1 µmol) was added to the cells at different incubation time intervals (2 and 4 h) in dark. Then the cells were trypsinized, transferred into 1.5 ml centrifuge tubes, washed once with chilled PBS and fixed by

adding 800 µl of chilled 70% ethanol drop-wise with constant and gentle vortexing to prevent cell aggregation. The cell suspension was incubated at -20 °C for 6 h. The fixed cells were then washed twice with 1.0 ml of chilled PBS by centrifuging at 4000 rpm for 5 min at 4° C. The supernatant was discarded and the cell pellet was suspended in 200 µl of PBS containing 10 µg ml^{-1} of DNAse-free RNAse for 12 h at 37° C for digesting the cellular RNA. After RNAse digestion cells were washed twice with DPBS. Flow cytometric analysis was performed using FACS Calibur (Becton Dickinson (BD) cell analyzer) at FL1 channel.

Fluorescence microscopy

HeLa and MCF-7 cells (4 x 10^4 cells/mm^2), plated on cover slips, were incubated with 10 µmol of complex **2** for 2 and 4 h in the dark, fixed with 4% paraformaldehyde for 10 min at room temperature (RT) and washed with PBS. This was followed by staining with Hoechst 33342 for 10 min at 25 °C. The cells were washed, mounted in 90% glycerol solution containing Mowiol, an anti-fade reagent, and sealed. Images were acquired using Apotome.2 fluorescence microscope (Carl Zeiss, Germany) using an oil immersion lens at 63 X magnification. The images were analyzed using the AxioVision Rel 4.8.2 (Carl Zeiss, Germany) software.[S20] To understand the sub-cellular localization of the complexes, HeLa and MCF-7 cells (4 x 10^4 cells/mm^2) were incubated with 10 µmol of complex **2** for 2 and 4 h in the dark, following which, the cells were treated with 500 nmol of ER-Tracker Red in serum-free medium for 30 min at 37 ºC. The cells were then washed with PBS, mounted on slides and sealed with nail-paint. The images were acquired using Apotome .2 fluorescence microscope at 63X magnification and analyzed using AxioVision Rel 4.8.2 for sub-cellular localization of the compound. A similar method was followed for the mitotracker red experiment using complex **2**.

Endoplasmic Reticulum (ER) isolation by subcellular fractionation and estimation of Vanadium in ER

HeLa cells were analysed for the localization of complex **2** post-treatment by subcellular fractionation. About $5x10^6$ cells were plated in a 90mm petridish in 10% DMEM and cultured overnight. Cells were either treated with 1% DMSO or 30 µmol complex **2** for 4 h in dark. After incubation, cells were harvested and washed with PBS. Cells were re-suspended in 500 µl of homogenizing buffer (250 mmol sucrose, 10 mmol HEPES, 1 mmol EDTA, 1 mmol DTT, 10 mmol $MgCl_2$, 1 mmol PMSF, 10 mmol KCl) and lysed by passing 50 times through a 26 gauge needle on ice. The cell lysate was centrifuged at 1,000g for 10 min at 4^oC followed by another centrifugation of the supernatant at 10,000g for 10 min at 4^oC. The resultant supernatant containing the ER was centrifuged at 100,000g for 90 min at 4^oC. The pellet was re-suspended in 100 µl of PBS and used for quantification of vanadium by! Inductively Coupled Plasma Mass Spectrometer (ICPMS, Thermo X Series II). Contamination of ER fraction with mitochondria and cytosol was checked using western blot.

References

(S1) D. D. Perrin, W. L. F. Armarego and D. R. Perrin, *Purification of Laboratory Chemicals*; Pergamon Press: Oxford, 1980.

(S2) M. Mariappan, M. Suenaga, A. Mukhopadhyay, P. Raghavaiah and B. G. Maiya, *Inorg. Chim. Acta*., 2011, **376**, 340-349.

(S3) (a) T. Mukherjee, J. C. Pessoa, A. Kumar and A. R. Sarkar, *Inorg. Chem.*, 2011, **50**, 4349-4361; (b) D. Sharma, S. K. Sahoo, S. Chaudhary, R. K. Bera and J. F. Callan, *Analyst*, 2013, **138**, 3646-3650.

(S4) (a) D. F. Evans, *J. Chem. Soc*., 1959, 2003-2005; (b) D. F. Evans and T. A. James, *J. Chem. Soc. Dalton Trans*., 1979, 723-726.

(S5) J. Guilford II, R. Jackson, C. Choi and W. R. Bergmark, *J. Phys. Chem*., 1985, **89**, 294-300.

(S6) J. R. Lakowicz, *Principles of Fluorescence Spectroscopy*, Kluwer Academic/Plenum Publishers, New York, 1999.

(S7) A. T. R. Williams, S. A. Winfield and J. N. Miller, *Analyst,* 1983, **108**, 1067-1071.

(S8) (a) S. Wolfgang, K. Holger, W. Dieter, H. Steffen, R. Beate and S. Gunter, *J. Porphyrins. Phthalocyanines*, 1998, **2**, 145−158. (b) N. Mark, S. P. Michael and C. W. Brian, *Photochem. Photobiol*., 2002, **75**, 382−391.

(S9) M. Sean, A. S. Trevor and P. G. Kenneth, *Photochem. Photobiol. Sci*., 2007, **6**, 995−1002.

(S10) N. Walker and D. Stuart, *Acta Crystallogr.*, 1983, **A39**, 158-166.

(S11) G. M. Sheldrick, *SHELX-97, Programs for Crystal Structure Solution and Refinement*; University of Göttingen, Göttingen, Germany, 1997.

(S12) J. L. Farrugia, *J. Appl. Crystallogr*., 1999, **32**, 837-838.

(S13) C. K. Johnson, *ORTEP, Report ORNL-5138*; Oak Ridge National Laboratory: Oak Ridge, TN, 1976.

(S14) (a) A. D. Becke, *Phys. Rev*., 1998, **A38**, 3098-3100; (b) A.D. Becke, *J. Chem. Phys*., 1993, **98**, 5648-5652; (c) C. Lee, W. Yang and R.G. Parr, *Phys. Rev., B*. 1988, **37**, 785-789; (d) P.J. Hay and W.R. Wadt, *J. Chem. Phys*., 1985, **82**, 284-298.

(S15) Gaussian 09, Revision A.02, M. J. Frisch, G. W. Trucks, H. B. Schlegel, G. E. Scuseria, M. A. Robb, J. R. Cheeseman, G. Scalmani, V. Barone, B. Mennucci, G. A. Petersson, H.Nakatsuji, M. Caricato, X. Li, H. P. Hratchian, A. F. Izmaylov, J. Bloino, G. Zheng, J. L.Sonnenberg, M. Hada, M. Ehara, K. Toyota, R. Fukuda, J. Hasegawa, M. Ishida, T.Nakajima, Y. Honda, O. Kitao, H. Nakai, T. Vreven, J. A. Montgomery, Jr., J. E. Peralta, F.Ogliaro, M. Bearpark, J. J. Heyd, E. Brothers, K. N. Kudin, V. N. Staroverov, R. Kobayashi,J. Normand, K. Raghavachari, A. Rendell, J. C. Burant, S. S. Iyengar, J. Tomasi, M. Cossi,N. Rega, J. M.

Millam, M. Klene, J. E. Knox, J. B. Cross, V. Bakken, C. Adamo, J. Jaramillo,R. Gomperts, R. E. Stratmann, O. Yazyev, A. J. Austin, R. Cammi, C. Pomelli, J. W.Ochterski, R. L. Martin, K. Morokuma, V. G. Zakrzewski, G. A. Voth, P. Salvador, J. J.Dannenberg, S. Dapprich, A. D. Daniels, O. Farkas, J. B. Foresman, J. V. Ortiz, J.Cioslowski, and D. J. Fox, Gaussian, Inc., Wallingford CT, 2009.

(S16) T. Mosmann, *J. Immunol. Methods.*, 1983, **65**, 55-63.

(S17) C. Soni and A. A. Karande, *Mol. Immunol*., 2010, **47**, 2458-2466.

(S18) A. S. Keston and R. Brandt, *Anal. Biochem*., 1965, **11**, 1-5.

(S19) T. Takanashi, Y. Ogura, H. Taguchi, M. Hashizoe and Y. Honda, *Invest. Ophthalmol. Vis. Sci*., 1997, **38**, 2721-2728.

(S20) J. L. McClintock and B. P. Ceresa, *Invest. Opthalmol. Vis. Sci*., 2010, **51**, 3455-3461.

Table S1. Selected bond distances (Å) and angles (°) for [VO(HL)(bpy)]ClO_4·EtOH (**1a**·EtOH) with e.s.d.s in the parentheses

V(1)-N(1)	2.319(2)	O(1)-V(1)-N(3)	102.47(10)
V(1)-N(2)	2.134(2)	O(2)-V(1)-N(1)	81.43(9)
V(1)-N(3)	2.089(2)	O(2)-V(1)-N(2)	95.20(9)
V(1)-O(1)	1.598(2)	O(2)-V(1)-N(3)	86.82(9)
V(1)-O(2)	1.957(2)	O(3)-V(1)-N(1)	81.08(8)
V(1)-O(3)	1.982(2)	O(3)-V(1)-N(2)	92.28(9)
O(1)-V(1)-O(2)	99.32(11)	O(3)-V(1)-N(3)	80.48(9)
O(1)-V(1)-O(3)	101.12(11)	N(1)-V(1)-N(2)	72.07(8)
O(2)-V(1)-O(3)	157.83(9)	N(1)-V(1)-N(3)	92.62(8)
O(1)-V(1)-N(1)	164.91(10)	N(2)-V(1)-N(3)	164.00(9)
O(1)-V(1)-N(2)	92.88(10)		

(a)

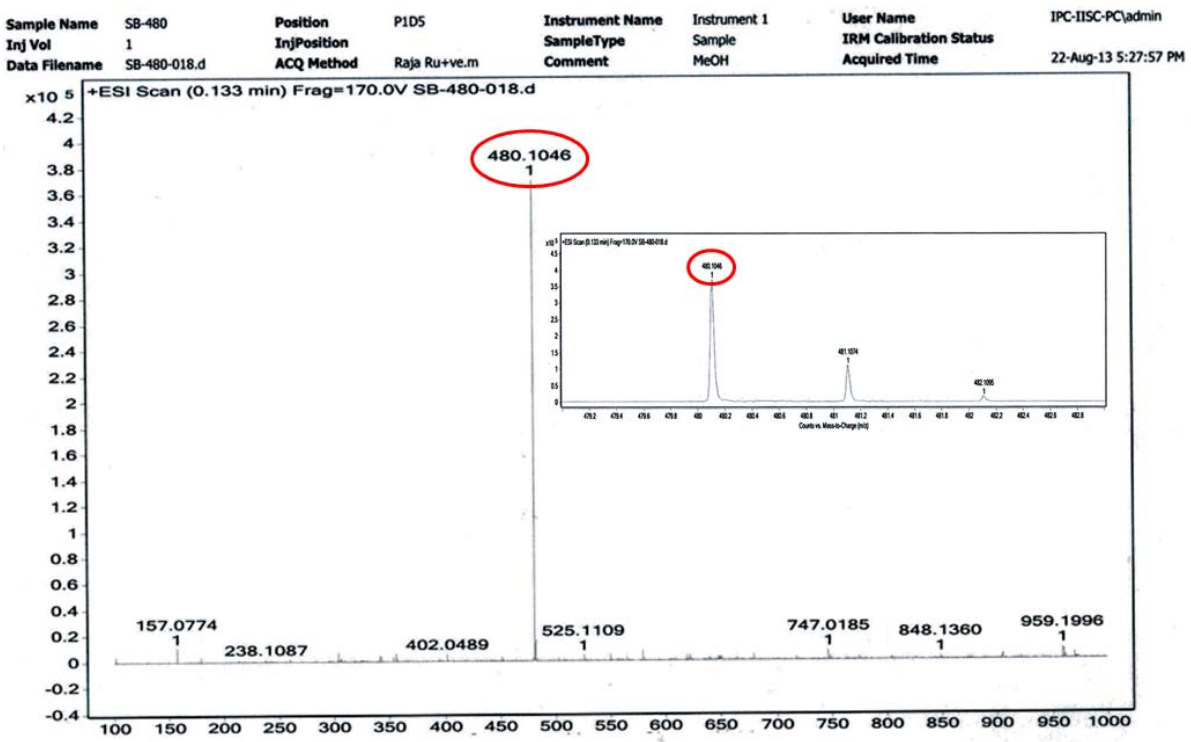

(b)

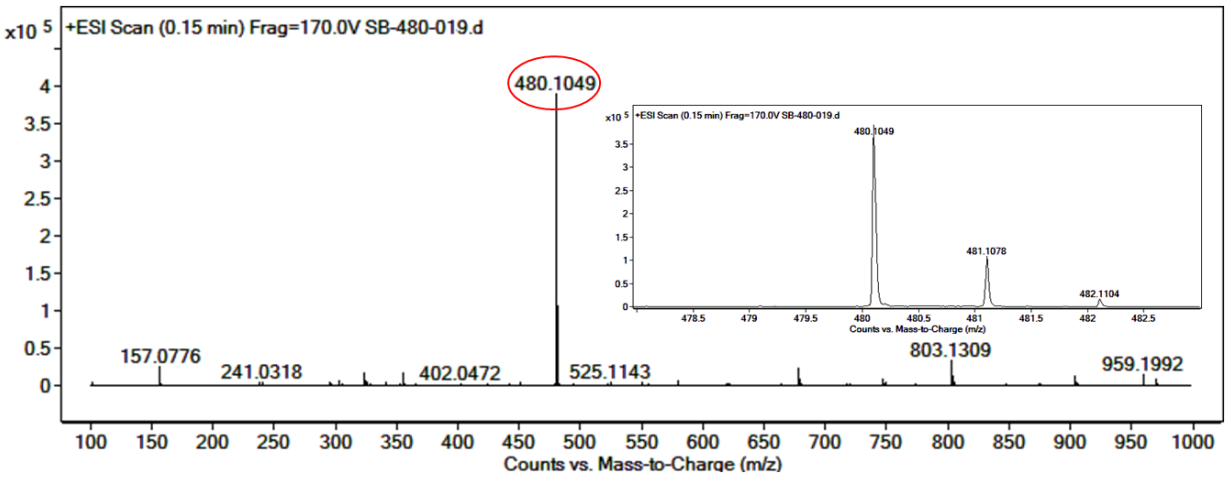

Fig. S1. The ESI-MS spectra of complex **1** showing the prominent $[M]^+$ peak in methanol (a) and aqueous methanol (1:1 v/v) (b) after keeping the solution for 48 h at 37 °C.

(a)

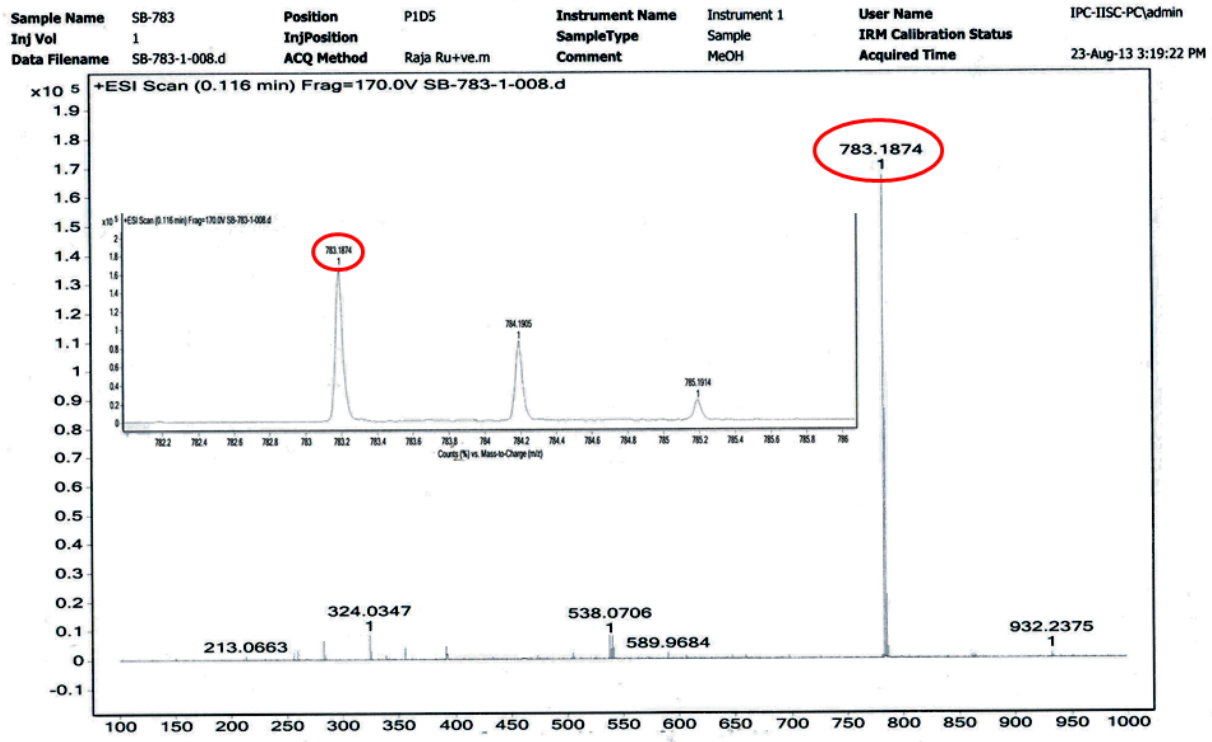

(b)

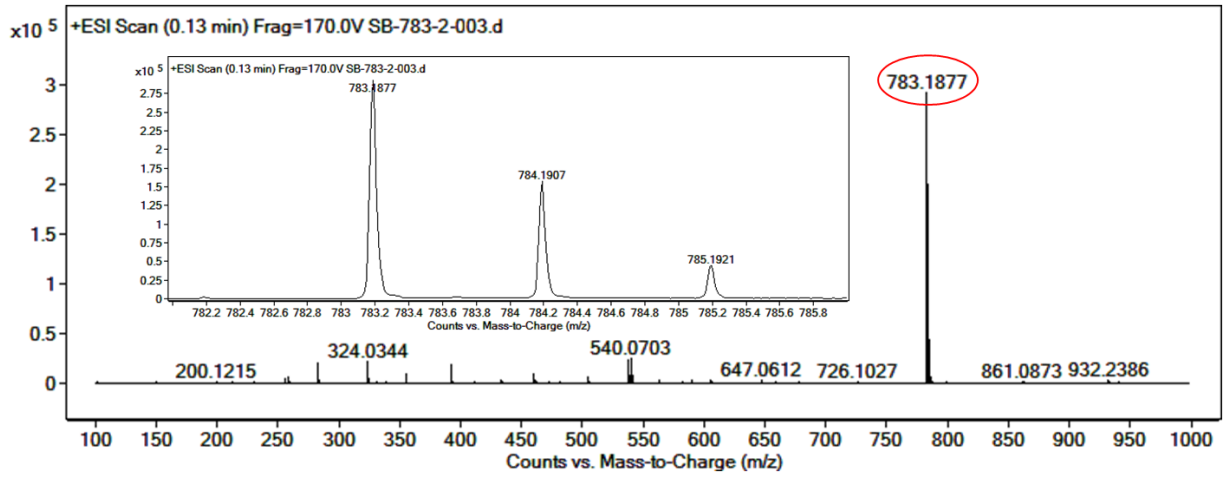

Fig. S2. The ESI-MS spectra of complex **2** showing the prominent $[M]^+$ peak in methanol (a) and after keeping the solution for 48 h at 37 °C in aqueous methanol (1:1 v/v) to ascertain its solution stability (b). The inset shows the isotropic distribution.

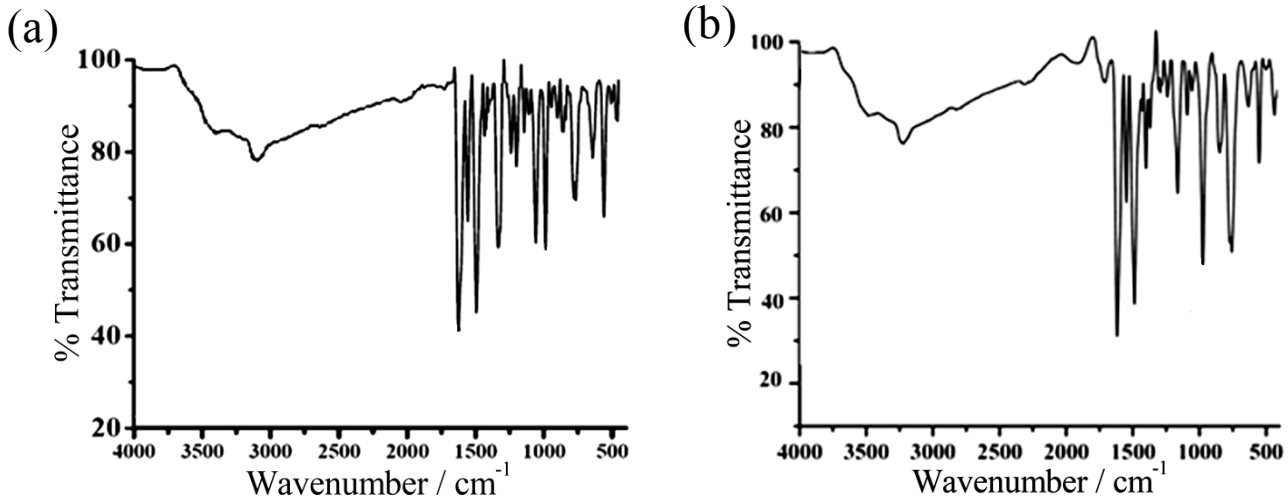

Fig. S3. IR spectra of complexes [VO(HL)(bpy)]Cl (**1**) (a) and [VO(HL)(acdppz)]Cl (**2**) (b).

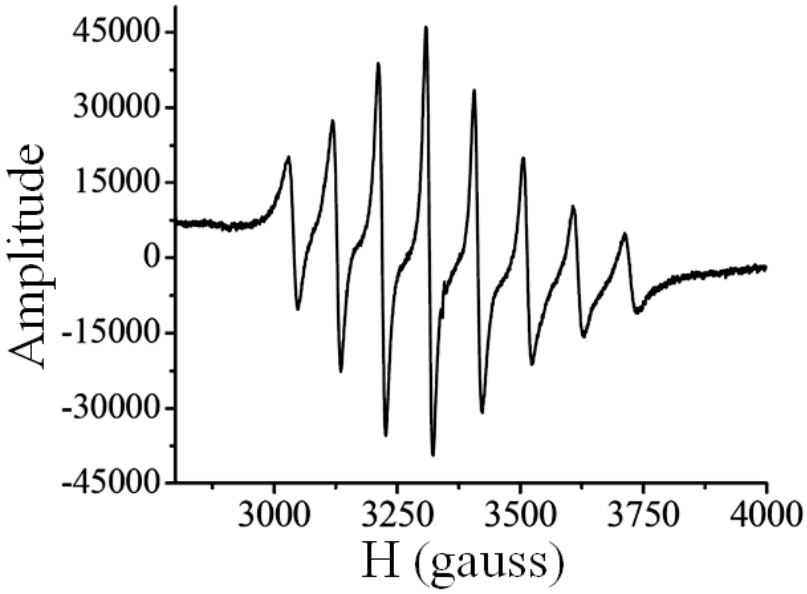

Fig. S4. EPR spectrum of complex **2** (5 mmol) in MeOH. The experimental conditions and operating frequency are: T = 298 K, ν = 9.40 GHz, modulation amplitude = 4.0 G at 100 kHz, and receiver gain = 1 x 10^{-3}. The signal is centered at g = 1.996 with hyperfine coupling constant in the region of 97.30 x 10^{-4} cm^{-1} indicating the existence of $3d^1$-vanadium(IV) center.

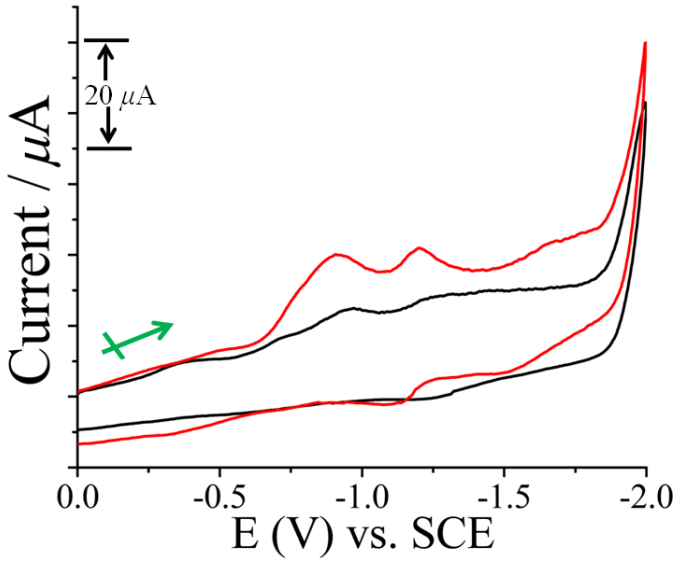

Fig. S5. Cyclic voltammograms of the complexes **1** (—) and **2** (—) showing the cathodic scan in 20% DMF-H_2O at a scan rate of 50 mV s^{-1} and 0.1 mol TBAP as the supporting electrolyte.

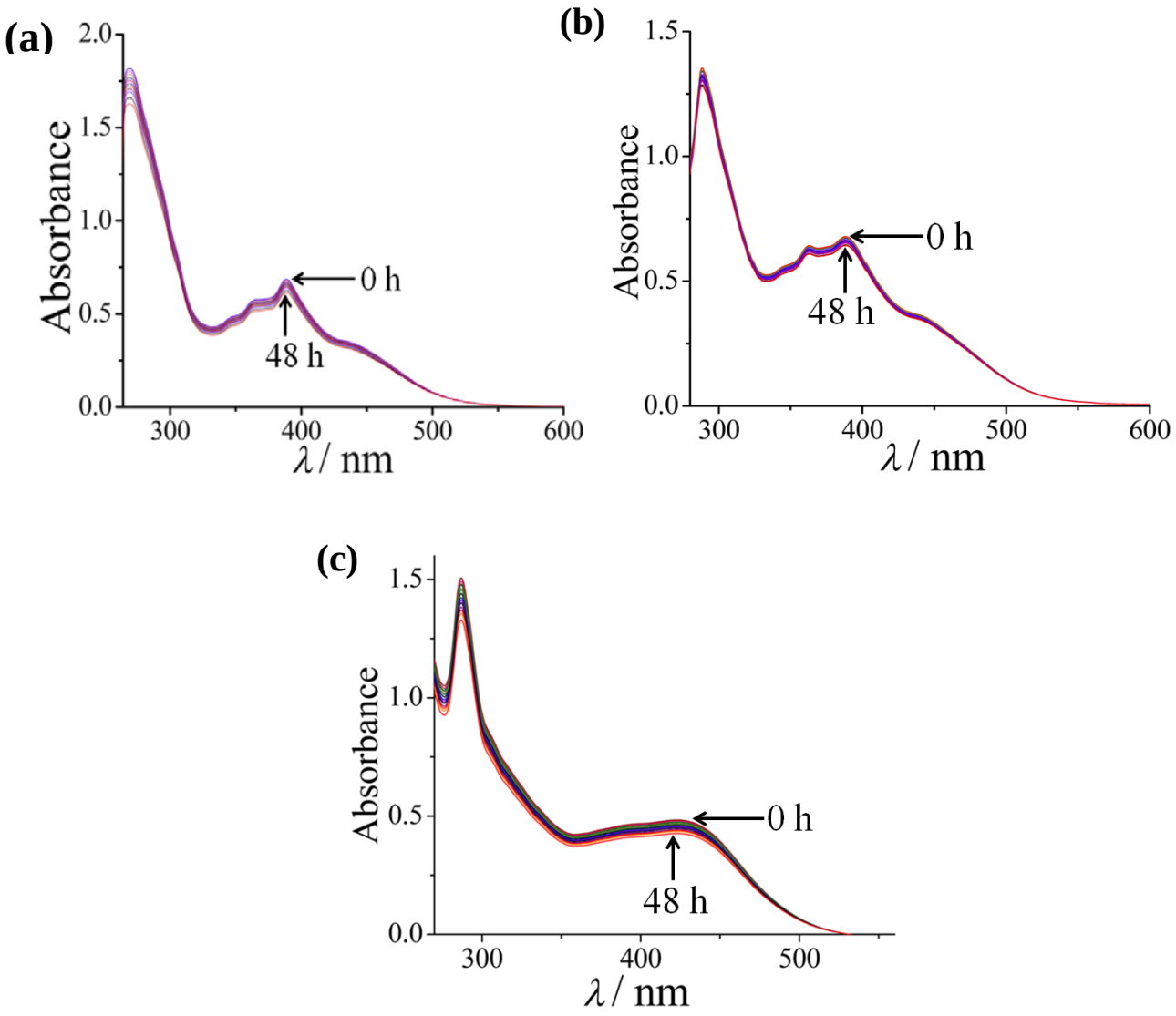

Fig. S6. Absorption spectral traces of complex **2** in DMSO-Tris buffer (1:2 v/v, pH = 6.8, 37 °C) (a) and in DMSO-10% DMEM medium (1:99 v/v, pH = 7.4, 37 °C) (b). (c) Absorption spectral traces of complex **1** in DMSO-10% DMEM medium (1:99 v/v, pH = 7.4, 37 °C). The spectra were recorded at interval of 20 min after keeping the solution at 37 °C and recorded at different time intervals. The spectral data indicate the stability of the complexes in the buffer and in cellular medium.

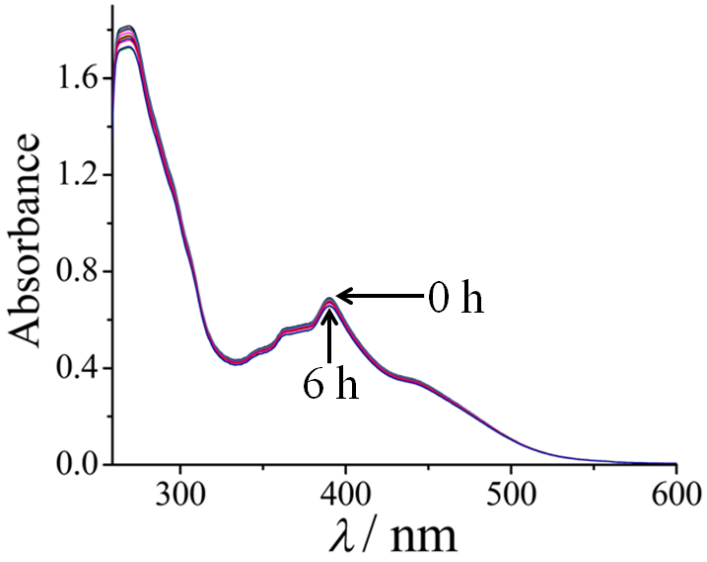

Fig. S7. Absorption spectral traces of complex **2** in DMSO- PBS (1:99 v/v, pH = 7.4, 37 °C). The spectra were recorded at interval of 30 min after irradiating the solution using the visible light of 400-700 nm (Luzchem Photoreactor: Model LZC-1, Ontario, Canada; light fluence rate: 2.4 mW cm^{-2}; light dose = 10 J cm^{-2}). The spectral data indicate that the complex **2** is photo-stable in the buffer medium even up to 6 h of irradiation.

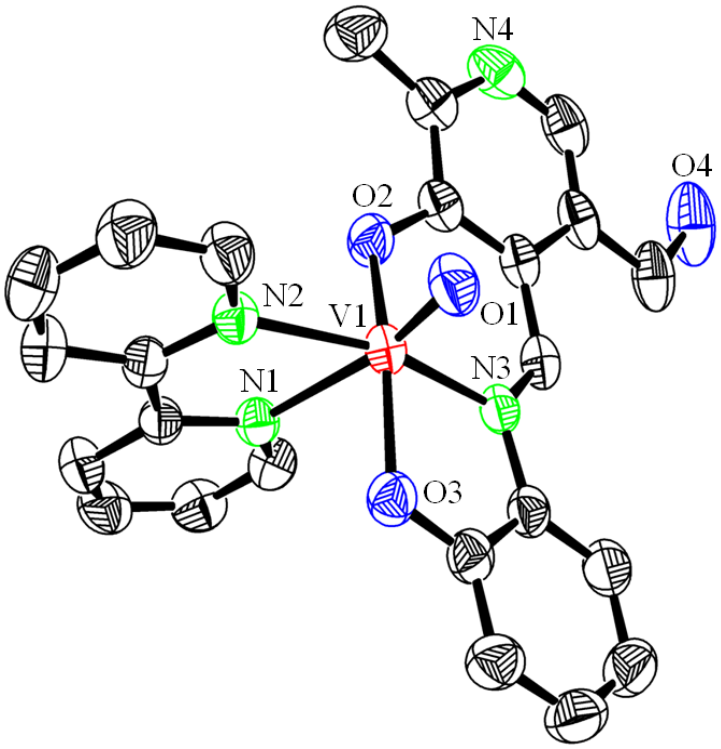

Fig. S8. An ORTEP view of the cationic complex in **1a** showing the atom labeling scheme for the metal and hetero atoms and 50% probability thermal ellipsoids. The hydrogen atoms, perchlorate anion and the lattice ethanol molecule are not shown for clarity.

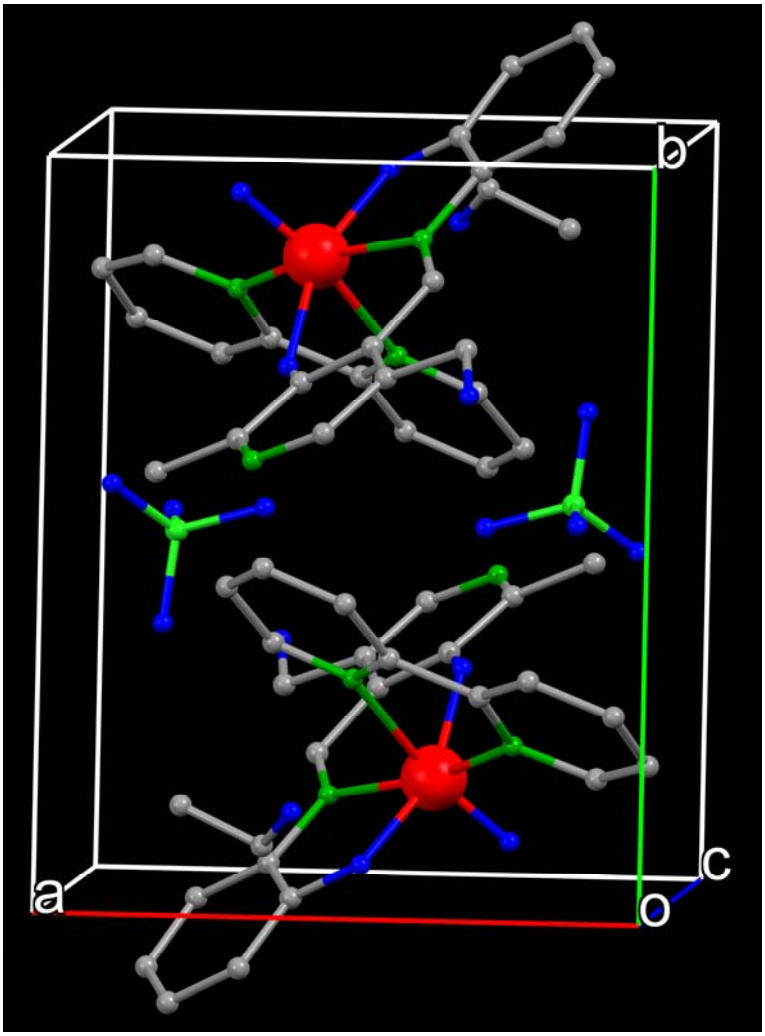

Fig. S9. The unit cell packing diagram of **1a**·EtOH with two complexes in the unit cell.

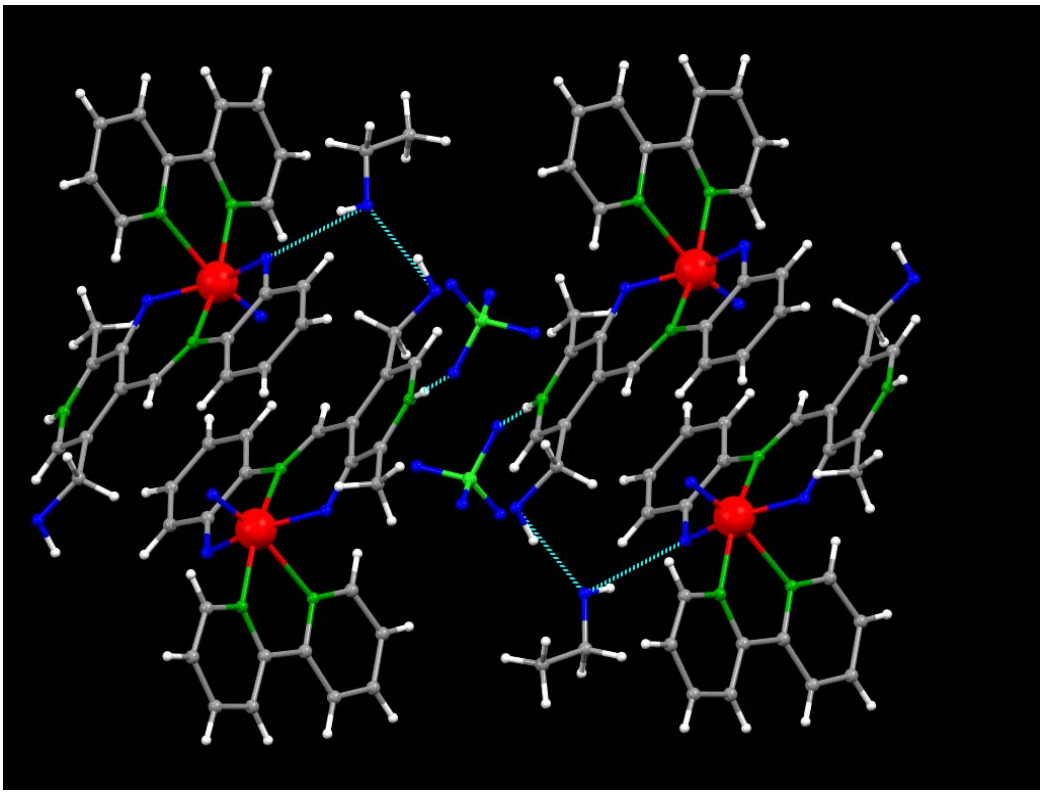

Fig. S10. The chemically significant H-bonding networks shown by dotted lines in the lattice of **1a**·EtOH.

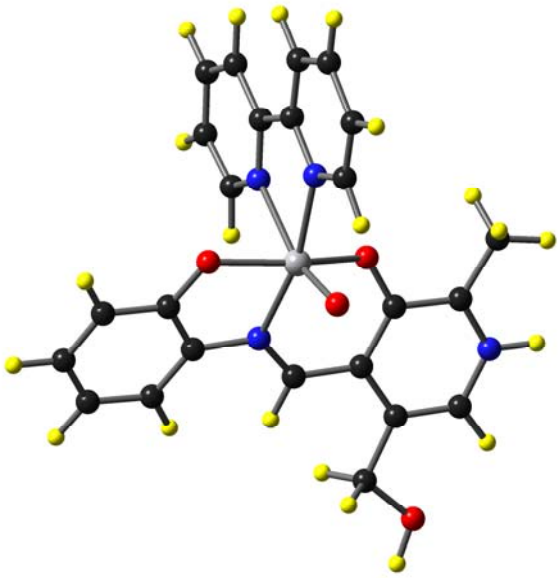

Fig. S11. The energy-optimized structure of the complex in **1** with color codes: C, black; N, blue; O, red; V, grey and H, yellow.

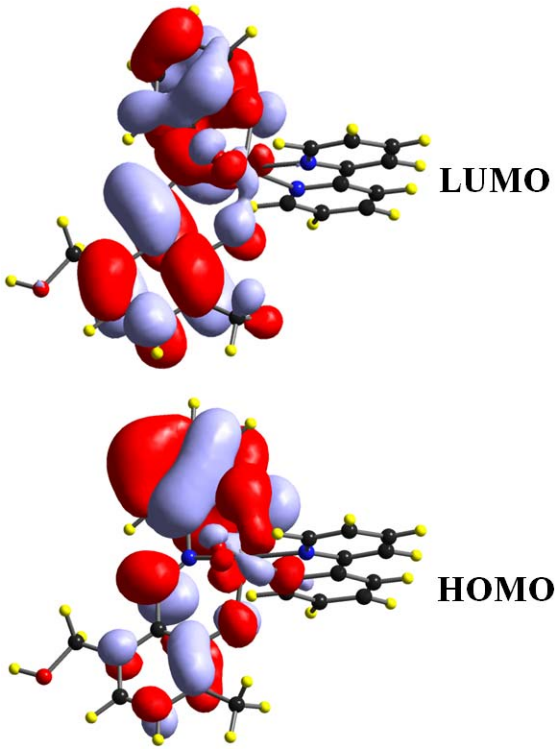

Fig. S12. The HOMO and LUMO of complex **1**.

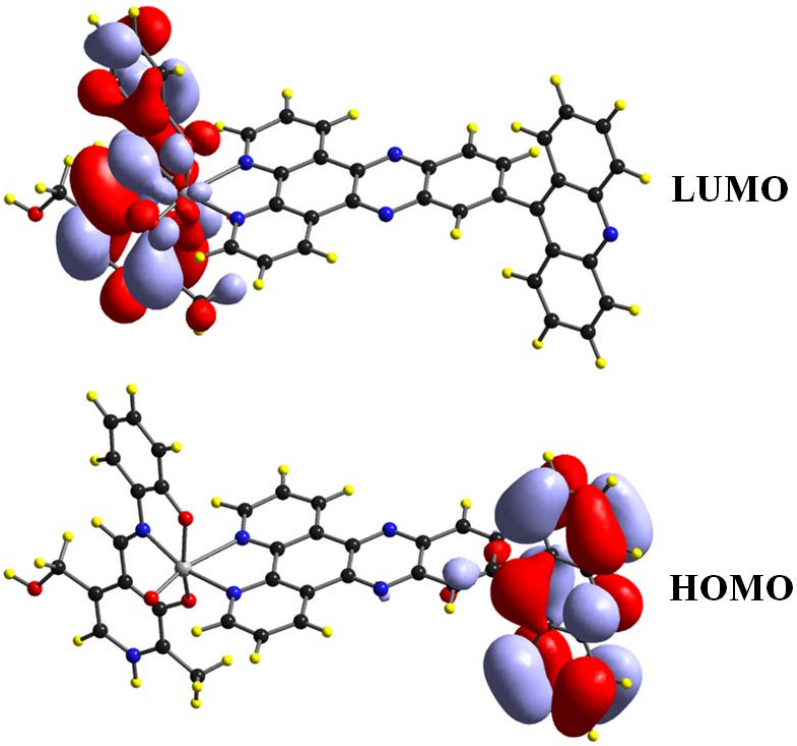

Fig. S13. The HOMO and LUMO of complex **2**.

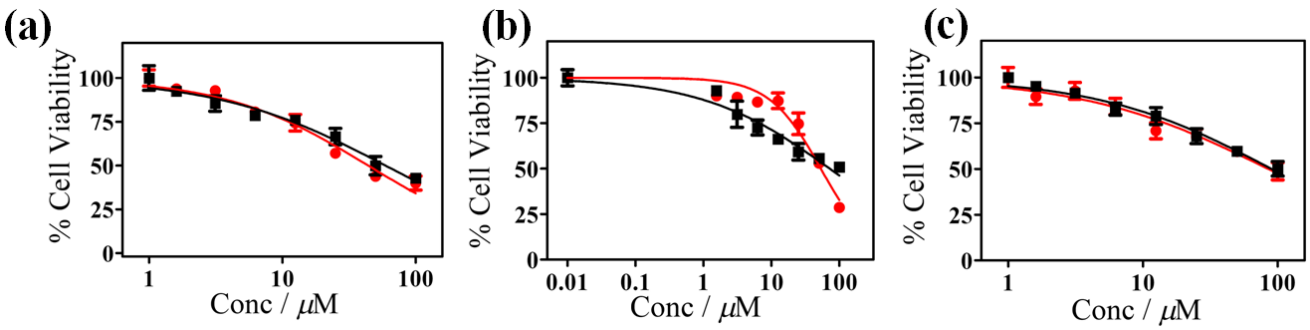

Fig. S14. Photocytotoxicity of the 2,2'-bipyridine complex **1** in HeLa (a), MCF-7 (b) and MCF-10A (c) cell lines on 4 h incubation in dark followed upon photo-irradiation in visible light (400 to 700 nm) for 1 h as determined by MTT assay. The photo-exposed and dark-treated cells are shown in red and black colour symbols, respectively. There is no apparent PDT effect of this photo-inactive complex in these cell lines.

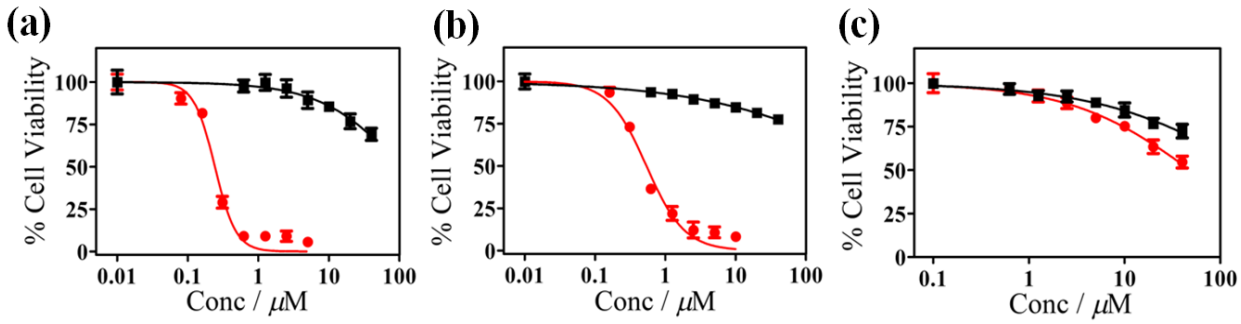

Fig. S15. Photocytotoxicity of complex **2** in HeLa (a), MCF-7 (b) and MCF-10A (c) cell lines on 4 h incubation in dark followed by photo-irradiation in visible light (400-700 nm) for 1 h as determined by MTT assay. The photo-exposed and dark-treated cells are shown in red and black colour symbols, respectively. Significant PDT effect is clearly visible in HeLa and MCF-7 cells [(a) and (b)]. There is no apparent PDT effect in MCF-10A cells (c).

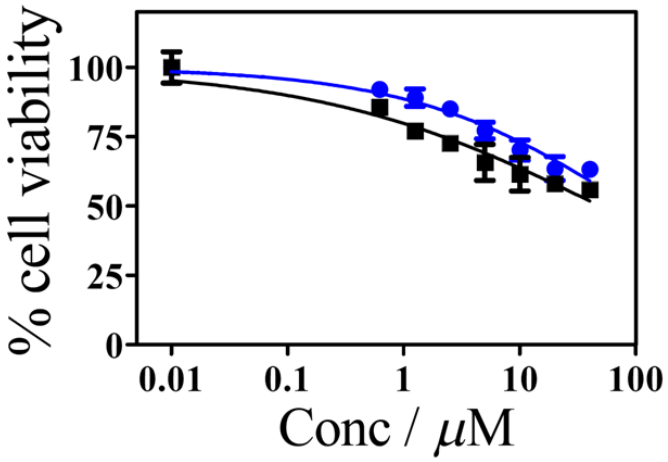

Fig. S16. Dark-toxicity of complex **2** in HeLa on 24 h and 48 h incubation in dark as determined by MTT assay. The 24 h and 48 h incubated cells are shown in blue and black colour symbols, respectively. The complex **2** is significantly non toxic in dark even after 48 h incubation.

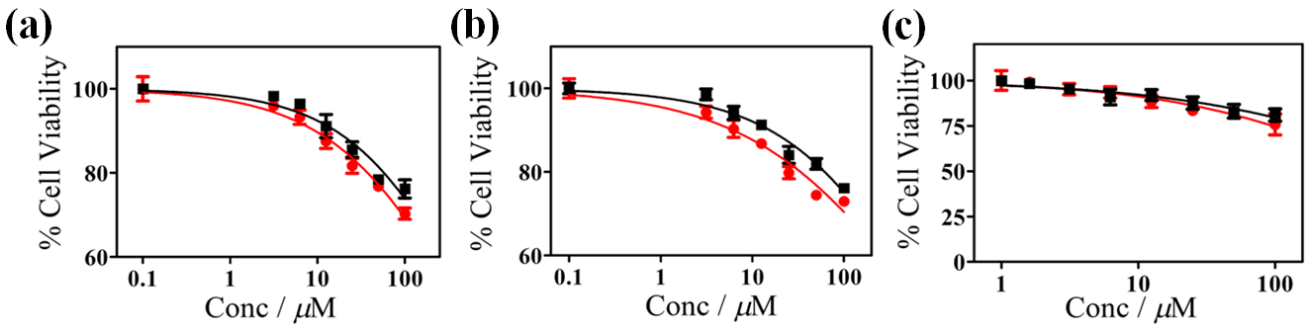

Fig. S17. Cell viability plots showing no significant photocytotoxicity of the vitamin B6 Schiff base ligand ($H_2L.HCl$) alone in HeLa (a), MCF-7 (b) and MCF-10A (c) cell lines on 4 h incubation in dark followed by exposure to visible light (400-700 nm, 10 J cm^{-2}) for 1 h, as determined from the MTT assay. Red and black colour symbols indicate data in visible light and in dark, respectively.

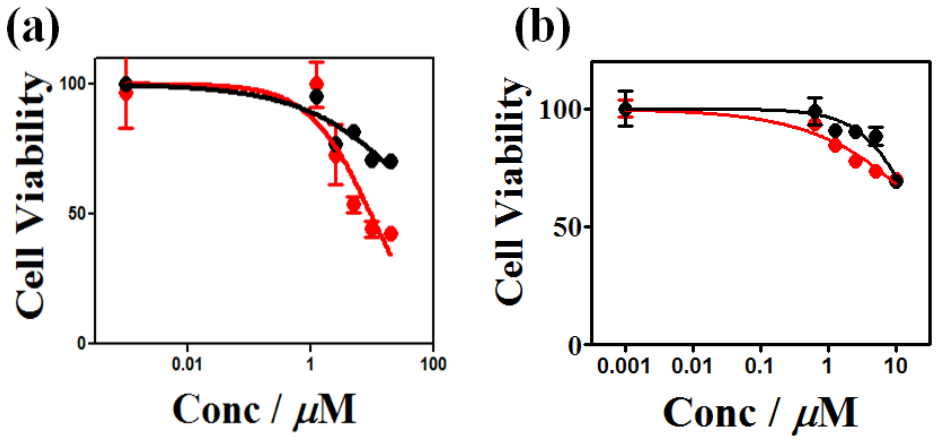

Fig. S18. Photocytotoxicity of the acdppz ligand alone in HeLa (a) and MCF-7 (b) cells upon incubation for 4 h in dark followed by irradiation with visible light (400-700 nm, 10 J cm^{-2}) for 1 h as determined by MTT assay. The photo-exposed and dark-treated cells are shown in red and black colour symbols, respectively. There is no significant PDT effect of this ligand alone when compared to that of complex **2**.

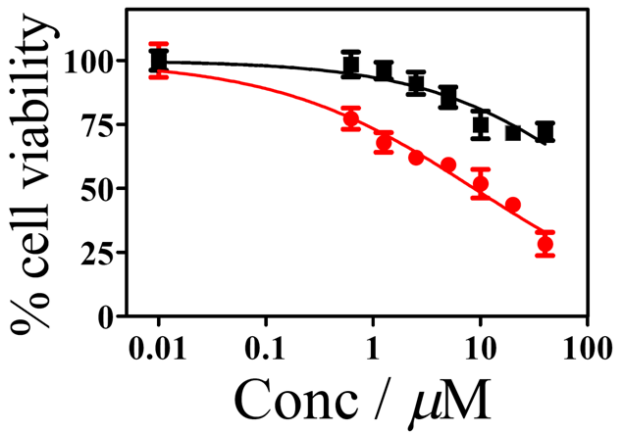

Fig. S19. Photocytotoxicity of complex **2** in HeLa cancer cells in the presence of Vit-B6. Cells were first incubated with 4 mmol Vit-B6 for 45 min followed by addition of complex **2** for the MTT assay. The photo-exposed and dark-treated cells are shown in red and black colour symbols, respectively. Significant decrease in the PDT effect was observed in HeLa which clearly indicates the Vit-B6 Schiff base in complex **2** contributes mostly towards cellular uptake.

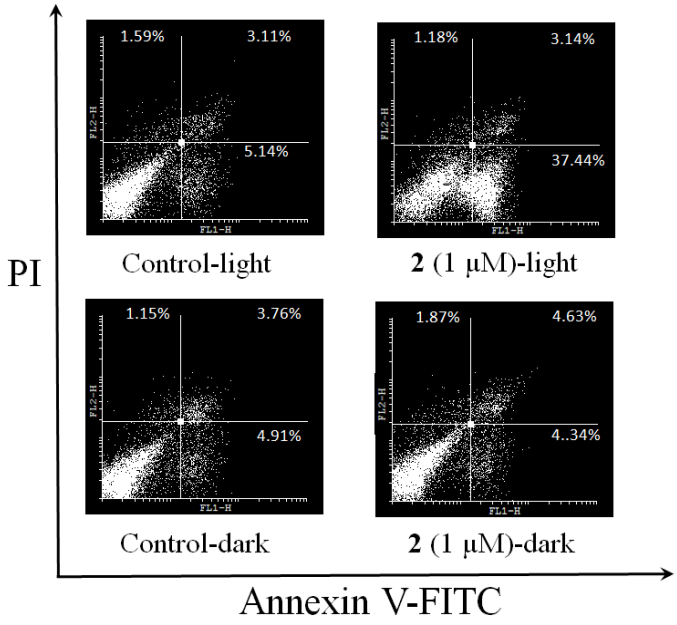

Fig. S20. FACScan profiles of Annexin-V FITC and propidium iodide (PI) staining of HeLa cells undergoing early apoptosis induced by complex **2** in dark and in visible light (400-700 nm).

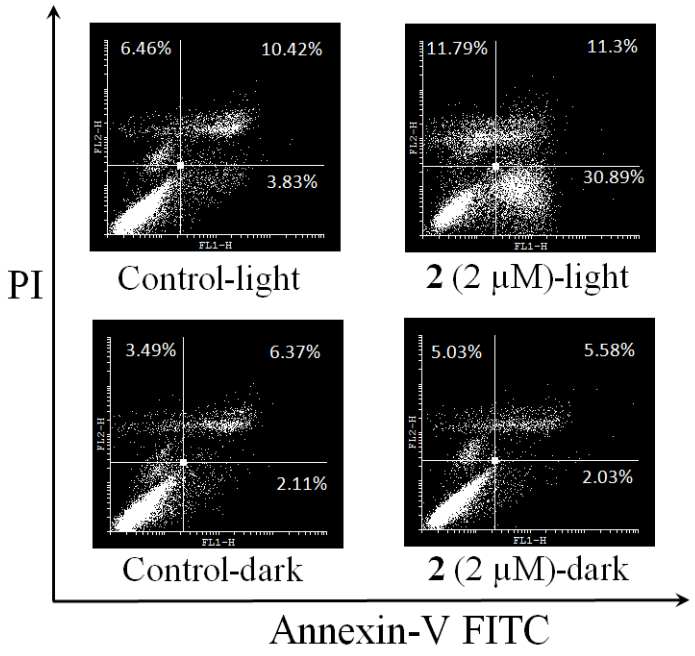

Fig. S21. FACScan profiles of Annexin-V FITC and PI staining of MCF-7 cells undergoing early apoptosis induced by complex **2** in dark and in visible light (400-700 nm).

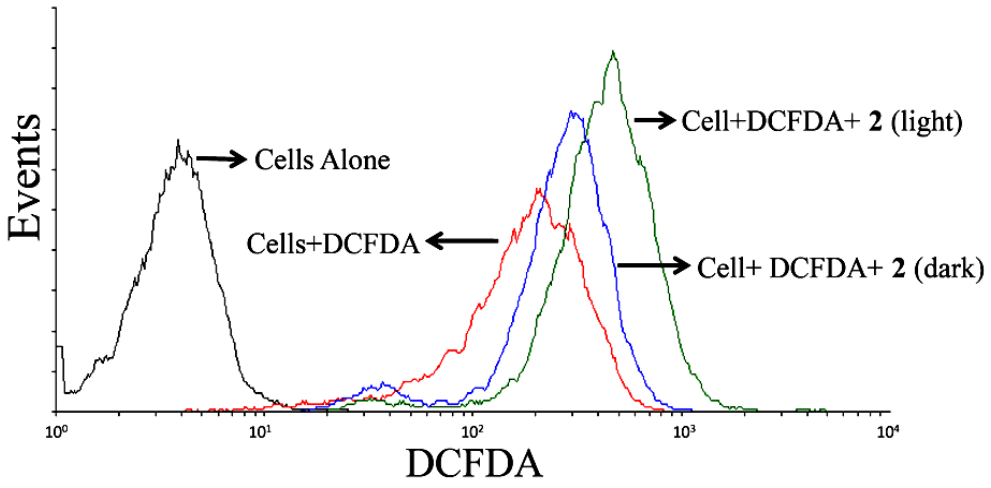

Fig. S22. Shift in band positions of complex **2** in HeLa cells in light of 400-700 nm (10 J cm^{-2}). Color code: black, cells only; red, cells + DCFDA; blue, cells + DCFDA + **2** (in dark); green, cells + DCFDA + complex **2** (in light).

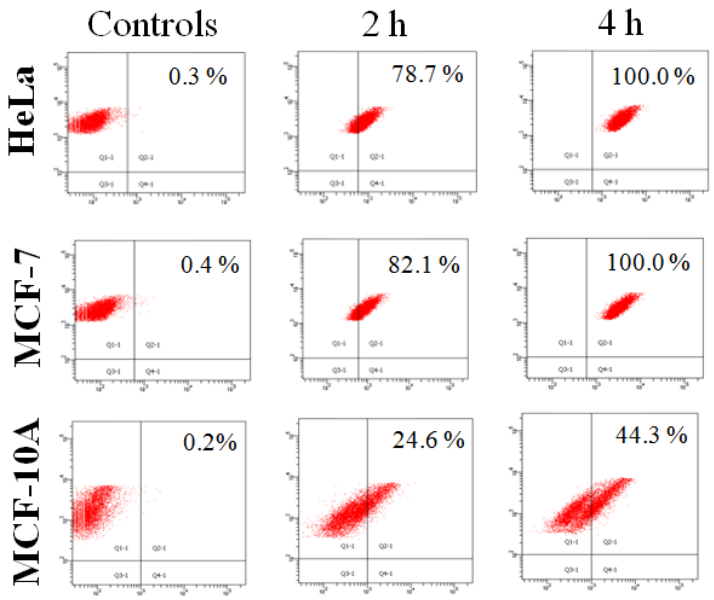

Fig. S23. A comparison of the cellular uptake of complex **2** (1 μmol) at 2 h and 4 h of incubation with HeLa, MCF-7 and MCF-10A cells as determined from the flow cytometric analysis.

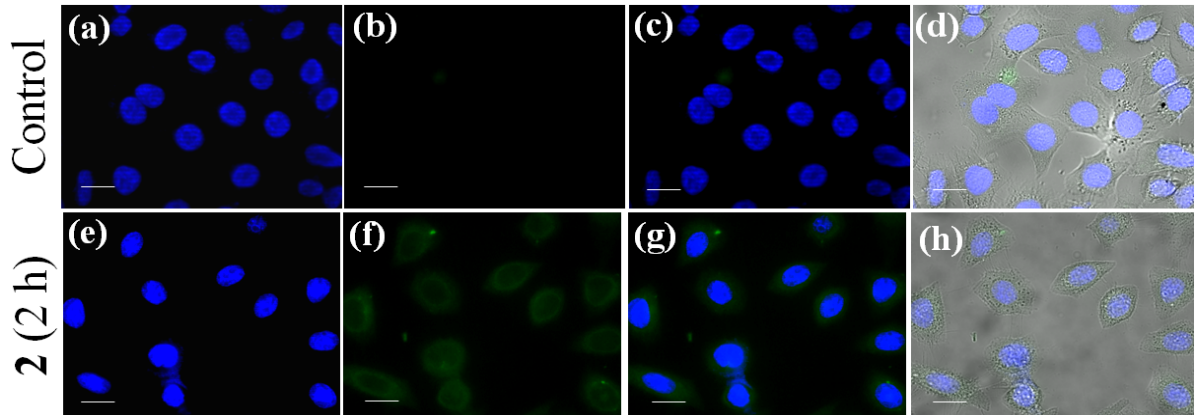

Fig. S24. Fluorescence microscopic images of HeLa cells [control and treated with complex **2** (10 μmol)] on 2 h incubation and Hoechst 33342 dye (5 μg m^{-1}). Panels (a, e) show the blue emission of Hoechst 33342 dye which stains the nucleus. Panel (b) is of the control. Panel (f) shows the green emission of complex **2**. Panels (c, g) correspond to the merged images showing cytosolic localization of the complex. Panels (d, h) show the control and complex treated bright field images. The cytosolic localization of **2** is visible in panels (f, g, h). Scale bar = 20 μm.

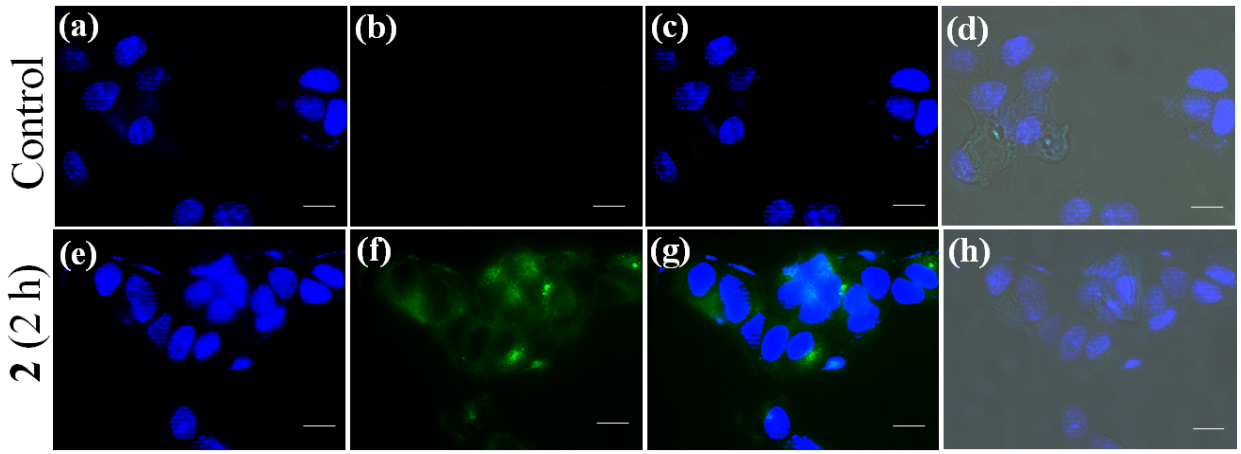

Fig. S25. Fluorescence microscopic images of MCF-7 cells [control and treated with complex **2** (10 μmol)] on 2 h incubation and Hoechst 33342 dye (5 μg m^{-1}). Panels (a, e) show the blue emission of Hoechst 33342 dye staining the nucleus. Panel (f) shows the green emission of **2**. Panels (c, g) correspond to the merged images showing cytosolic localization of the complex. Panels (d, h) show the control and complex treated bright field images. Scale bar: 20 μm.

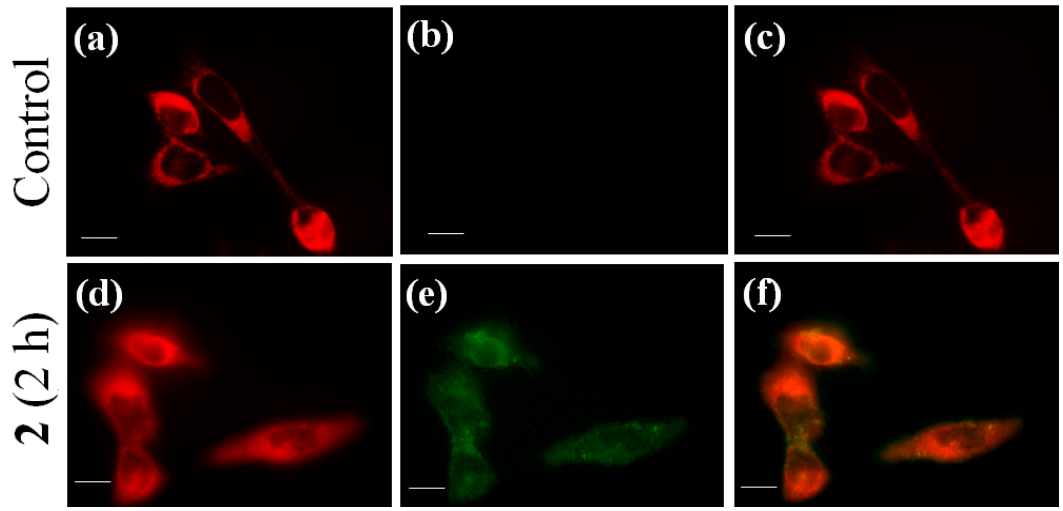

Fig. S26. Fluorescence microscopic images of complex **2** (10 μmol) and ER-tracker red (ERTR, 0.5 μmol) in HeLa cells after 2 h incubation showing their cellular uptake. Panels (a) and (d) show fluorescence of ERTR. Panels (e) is the fluorescence image of complex **2**. Panel (f) is the merged image of the ERTR and complex **2** showing localization of the complex in ER. Scale bar: 20 μm.

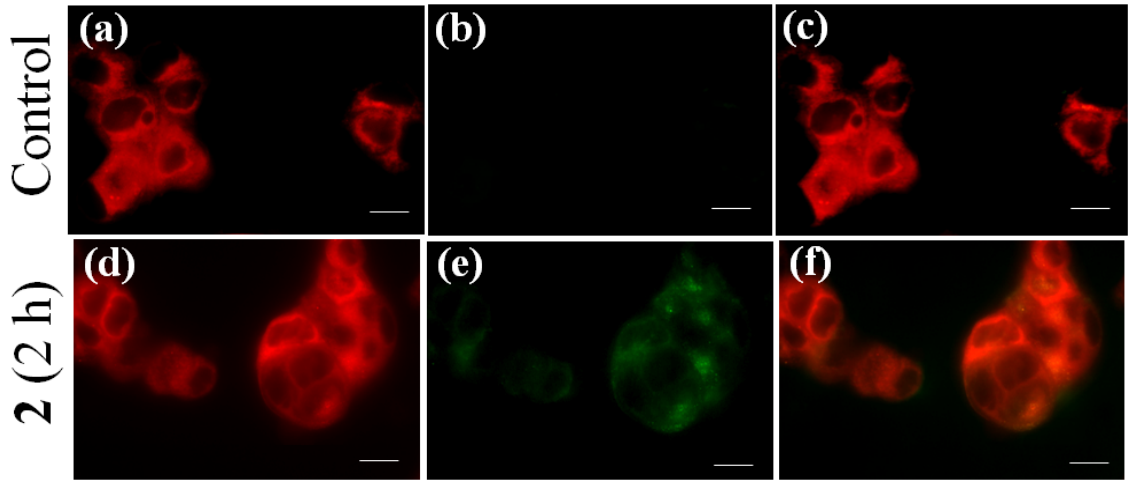

Fig. S27. Fluorescence microscopic images of MCF-7 cancer cells treated with complex **2** (10 μmol) and the ER-tracker red (ERTR, 0.5 μmol) after 2 h of incubation showing their cellular uptake. Panels (a) and (d) show the fluorescence of ERTR. Panel (e) is the fluorescence image of complex **2**. Panel (f) is the merged image of the ERTR and complex **2** showing localization of the complex in ER. Scale bar: 20 μm.

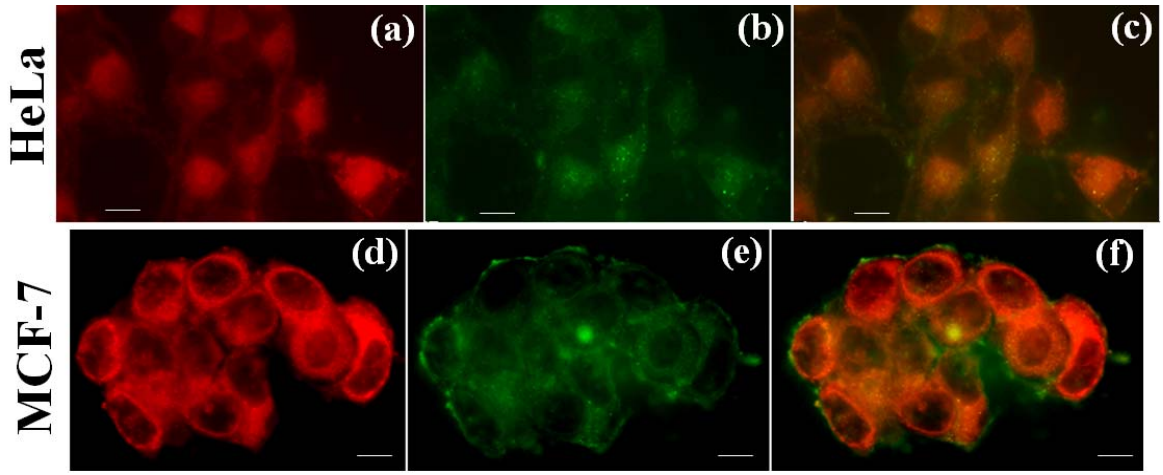

Fig. S28. Fluorescence microscopic images of HeLa and MCF-7 cells treated with complex **2** (10 μmol) and MitoTracker Red (MTR, 0.05 μmol) after 4 h of incubation showing their cellular uptake. Panels (a) and (d) show red fluorescence of MTR. Panels (b) and (e) display the fluorescence images of complex **2** with green emission. Panels (c) and (f) are the merged images of the MTR and complex **2**. The merged images indicate no apparent localization of complex **2** in the mitochondria even after 4 h of incubation. Scale bar: 20 μm

Table S2 : Computational data for complex **1**

Center Number	Atomic Number	Atomic Type	Coordinates (Angstroms) X	Y	Z
1	23	0	-0.553951	-0.037015	-0.785954
2	8	0	-0.109140	-0.437572	-2.275817
3	8	0	0.505318	-1.426653	0.175749
4	8	0	-1.476485	1.662424	-0.938363
5	8	0	6.498331	-0.257479	-0.011199
6	7	0	-1.586497	-0.000420	1.273637
7	7	0	-2.414676	-1.059570	-1.009822
8	7	0	1.023823	1.276263	-0.242341
9	7	0	3.688179	-3.061213	0.311771
10	6	0	-1.055859	0.541434	2.392714
11	1	0	-0.045832	0.928410	2.313408
12	6	0	-1.765634	0.607074	3.602725
13	1	0	-1.309140	1.054924	4.479063
14	6	0	-3.071210	0.083552	3.643093
15	1	0	-3.651779	0.117791	4.560141
16	6	0	-3.617796	-0.486904	2.481967
17	1	0	-4.620712	-0.897225	2.502769
18	6	0	-2.846804	-0.514835	1.302327
19	6	0	-3.313578	-1.097606	0.021777
20	6	0	-4.589927	-1.663686	-0.154489
21	1	0	-5.300559	-1.686955	0.663297
22	6	0	-4.944834	-2.196382	-1.404281
23	1	0	-5.928404	-2.631818	-1.553542
24	6	0	-4.011944	-2.153851	-2.455366
25	1	0	-4.245085	-2.550780	-3.437360
26	6	0	-2.756554	-1.574686	-2.219895
27	1	0	-1.999417	-1.501754	-2.991881
28	6	0	-0.757881	2.773947	-0.713729
29	6	0	-1.299389	4.076611	-0.864203
30	1	0	-2.331130	4.175120	-1.185725
31	6	0	-0.501593	5.189507	-0.595218
32	1	0	-0.918096	6.187509	-0.704882
33	6	0	0.851812	5.041062	-0.173483
34	1	0	1.449909	5.922037	0.039557
35	6	0	1.405409	3.769395	-0.031993
36	1	0	2.436063	3.673823	0.300207
37	6	0	0.611090	2.624540	-0.306781
38	6	0	2.278354	0.904275	-0.050371
39	1	0	3.039012	1.679689	0.022840
40	6	0	2.741641	-0.465849	0.051147
41	6	0	1.818039	-1.569404	0.165151
42	6	0	2.338260	-2.893494	0.297561
43	6	0	1.432251	-4.082452	0.408844
44	1	0	1.989988	-5.019794	0.519199
45	1	0	0.792588	-4.151951	-0.479220
46	1	0	0.756681	-3.966244	1.264238
47	6	0	4.598612	-2.040138	0.202646
48	1	0	5.651463	-2.280522	0.213996
49	6	0	4.149245	-0.734987	0.073098
50	6	0	5.187594	0.365951	-0.067062
51	1	0	5.041925	0.889928	-1.025120
52	1	0	5.074810	1.097422	0.749705
53	1	0	4.045784	-4.010341	0.401321
54	1	0	7.217007	0.392450	-0.147809

Table S3 : Computational data for complex **2**

Center Number	Atomic Number	Atomic Type	Coordinates (Angstroms) X	Y	Z
1	23	0	-3.997204	0.169204	1.118269
2	8	0	-4.634742	-0.353378	2.494381
3	8	0	-4.370422	-1.456779	0.029805
4	8	0	-3.640650	2.057320	1.383489
5	8	0	-10.308176	-2.016132	-1.295070
6	7	0	-2.602035	0.563879	-0.719422
7	7	0	-2.024703	-0.305627	1.762645
8	7	0	-5.701464	0.989852	0.157711
9	7	0	-6.843231	-3.913720	-0.786093
10	6	0	-2.944852	0.988939	-1.949805
11	1	0	-4.004643	1.106411	-2.149884
12	6	0	-1.979859	1.274565	-2.942583
13	1	0	-2.300796	1.620849	-3.919303
14	6	0	-0.623939	1.107894	-2.644567
15	1	0	0.153743	1.315953	-3.371234
16	6	0	-0.251054	0.653624	-1.356516
17	6	0	-1.282097	0.393863	-0.422813
18	6	0	-0.970440	-0.077401	0.919184
19	6	0	0.369983	-0.284185	1.317603
20	6	0	0.612985	-0.738714	2.635927
21	1	0	1.637919	-0.896667	2.953088
22	6	0	-0.470729	-0.966593	3.488920
23	1	0	-0.323086	-1.310679	4.506685
24	6	0	-1.781589	-0.738788	3.020935
25	1	0	-2.653660	-0.892557	3.646249
26	6	0	-4.566252	2.923013	0.942029
27	6	0	-4.459264	4.323571	1.142987
28	1	0	-3.600576	4.705066	1.685847
29	6	0	-5.449060	5.169290	0.640729
30	1	0	-5.364250	6.242625	0.790057
31	6	0	-6.570016	4.650491	-0.070628
32	1	0	-7.322588	5.329456	-0.460373
33	6	0	-6.699085	3.276360	-0.267406
34	1	0	-7.555775	2.898056	-0.819517
35	6	0	-5.705331	2.398714	0.241993
36	6	0	-6.717929	0.281560	-0.304628
37	1	0	-7.621984	0.812004	-0.598999
38	6	0	-6.744197	-1.161888	-0.440361
39	6	0	-5.553197	-1.960244	-0.269980
40	6	0	-5.638778	-3.374534	-0.455589
41	6	0	-4.441001	-4.259391	-0.284717
42	1	0	-4.671277	-5.312270	-0.485545
43	1	0	-4.049461	-4.169790	0.735789
44	1	0	-3.633244	-3.936704	-0.951721
45	6	0	-7.997900	-3.191030	-0.952501
46	1	0	-8.907079	-3.716610	-1.204556
47	6	0	-7.972253	-1.814782	-0.786691
48	6	0	-9.275124	-1.051513	-0.959652
49	1	0	-9.519746	-0.522978	-0.024512
50	1	0	-9.170716	-0.304899	-1.763714
51	1	0	-6.891179	-4.923154	-0.910276
52	1	0	-11.188236	-1.595158	-1.371382
53	6	0	5.796177	0.566485	-1.981238
54	6	0	4.485999	0.768235	-2.380787
55	6	0	3.416719	0.506189	-1.472591
56	6	0	3.728379	0.027558	-0.140269
57	6	0	5.087719	-0.179376	0.235330
58	6	0	6.117941	0.083100	-0.661301
59	1	0	6.610860	0.760029	-2.673433
60	1	0	4.239820	1.122874	-3.376504
61	1	0	5.291594	-0.534770	1.240243
62	6	0	1.455721	-0.021422	0.366946

63	6	0	1.145851	0.449053	-0.966092
64	7	0	2.726256	-0.227859	0.759366
65	7	0	2.119053	0.704467	-1.860848
66	6	0	7.551078	-0.133628	-0.286566
67	6	0	8.054945	-1.446966	-0.071048
68	6	0	8.432103	0.975516	-0.153972
69	6	0	7.263781	-2.642246	-0.210047
70	6	0	9.459943	-1.594684	0.280207
71	6	0	9.820755	0.715247	0.192311
72	6	0	8.019553	2.345332	-0.316594
73	6	0	7.817609	-3.890805	0.003961
74	1	0	6.220267	-2.558962	-0.497318
75	6	0	9.996944	-2.909249	0.501777
76	6	0	10.731138	1.818259	0.331043
77	1	0	6.980733	2.566657	-0.542568
78	6	0	8.923392	3.381703	-0.170467
79	6	0	9.199146	-4.029024	0.370553
80	1	0	7.206533	-4.782736	-0.110525
81	1	0	11.047298	-2.974760	0.767723
82	6	0	10.297544	3.117614	0.151502
83	1	0	11.759466	1.581330	0.585355
84	1	0	8.594655	4.410630	-0.293418
85	1	0	9.611969	-5.020657	0.536140
86	1	0	10.990128	3.948083	0.259799
87	7	0	10.305002	-0.537405	0.402299